

Reappearance of linear hole transport in an ambipolar undoped GaAs/AlGaAs quantum well

This content has been downloaded from IOPscience. Please scroll down to see the full text.

2017 J. Phys.: Condens. Matter 29 185302

(<http://iopscience.iop.org/0953-8984/29/18/185302>)

View [the table of contents for this issue](#), or go to the [journal homepage](#) for more

Download details:

IP Address: 131.111.184.102

This content was downloaded on 18/05/2017 at 14:52

Please note that [terms and conditions apply](#).

You may also be interested in:

[N-type ohmic contacts to undoped GaAs/AlGaAs quantum wells using only front-sided processing: application to ambipolar FETs](#)

D Taneja, F Sfigakis, A F Croxall et al.

[Towards low-dimensional hole systems in Be-doped GaAs nanowires](#)

A R Ullah, J G Gluschke, P Krogstrup et al.

[Negative transconductance in parallel conducting systems controlled by device geometry and magnetic field](#)

I S Millard, N K Patel, E H Linfield et al.

[Low-dimensional quantum devices](#)

C G Smith

[Interactions in 2D electron and hole systems](#)

Y Y Proskuryakov, A K Savchenko, S S Safonov et al.

[The 0.7 anomaly in one-dimensional hole quantum wires](#)

A R Hamilton, R Danneau, O Klochan et al.

[Single-gated mobility modulation transistor](#)

P I Birjulin, Yu V Kopaev, V T Trofimov et al.

Reappearance of linear hole transport in an ambipolar undoped GaAs/AlGaAs quantum well

Deepyanti Taneja¹, Issai Shlimak², Vijay Narayan¹, Moshe Kaveh², Ian Farrer³ and David Ritchie¹

¹ Department of Physics, University of Cambridge, J J Thomson Avenue, Cambridge CB3 0HE, United Kingdom

² Jack and Pearl Resnick Institute of Advanced Technology, Department of Physics, Bar Ilan University, Ramat Gan 52900, Israel

³ Department of Electronic and Electrical Engineering, University of Sheffield, Mappin Street, Sheffield, S1 3JD, United Kingdom

E-mail: vn237@cam.ac.uk and shlimai@biu.ac.il

Received 23 December 2016, revised 23 February 2017

Accepted for publication 7 March 2017

Published 31 March 2017



Abstract

We report the results of an investigation of ambipolar transport in a quantum well of 15 nm width in an undoped GaAs/AlGaAs structure, which was populated either by electrons or holes using positive or negative gate voltage V_{tg} , respectively. More attention was focussed on the low concentration of electrons n and holes p near the metal–insulator transition (MIT). It is shown that the electron mobility μ_e increases almost linearly with increase of n and is independent of temperature T in the interval 0.3 K–1.4 K, while the hole mobility μ_p depends non-monotonically on p and T . This difference is explained on the basis of the different effective masses of electrons and holes in GaAs. Intriguingly, we observe that at low p the source–drain current (I_{SD})–voltage (V) characteristics, which become non-linear beyond a certain I_{SD} , exhibit a re-entrant linear regime at even higher I_{SD} . We find, remarkably, that the departure and reappearance of linear behaviour are not due to non-linear response of the system, but due to an intrinsic mechanism by which there is a reduction in the net number of mobile carriers. This effect is interpreted as evidence of inhomogeneity of the conductive 2D layer in the vicinity of MIT and trapping of holes in ‘dead ends’ of insulating islands. Our results provide insights into transport mechanisms as well as the spatial structure of the 2D conducting medium near the 2D MIT.

Keywords: non-linear I – V characteristics, two-dimensional hole gas, metal–insulator transition

(Some figures may appear in colour only in the online journal)

Ambipolar transport, or the ability to switch between electrons and holes in the same device, has strong implications towards the implementation of functional devices: for instance, creating gate-defined n - and p -type conducting channels in the same device can be exploited in thermoelectric

power generation, as well as towards spintronic applications by tuning between large (holes) and small (electrons) spin–orbit coupling. Equally, ambipolar transport is also of much interest in fundamental studies of scattering, interaction and spin related phenomena since electrons and holes have very different effective masses, band structures and spin properties [1, 2]. Chen *et al* [1] and Croxall *et al* [2] studied the density dependence of μ_p and μ_e in ambipolar GaAs/AlGaAs single heterojunction devices and quantum wells (QWs) respectively. The mobilities were found to depend not only on the



Original content from this work may be used under the terms of the Creative Commons Attribution 3.0 licence. Any further distribution of this work must maintain attribution to the author(s) and the title of the work, journal citation and DOI.

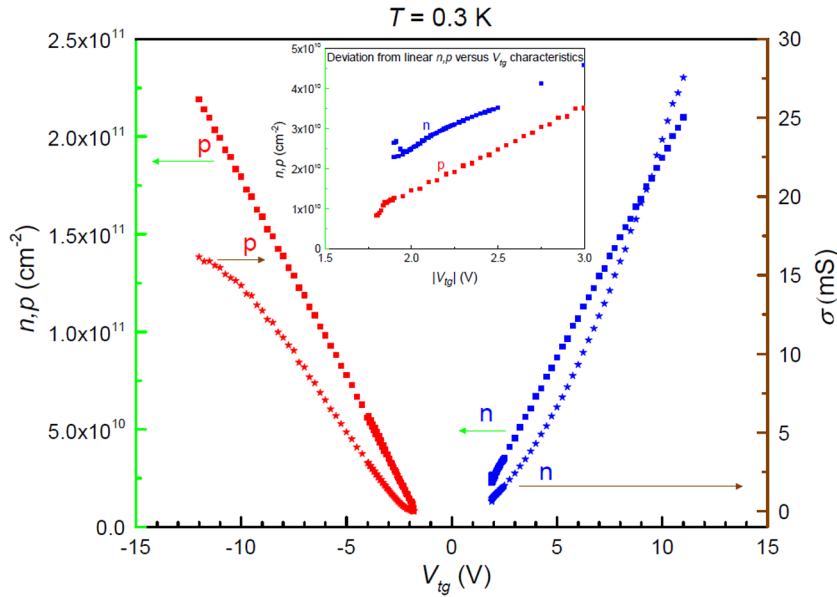


Figure 1. Carrier concentration n, p and conductivity σ as a function of top-gate voltage V_{tg} . The inset shows zoom-in of the low density end. Data taken with $I_{SD} = 100$ nA.

different effective masses m^* of electrons and holes but also on the different shapes of the electron and hole wavefunctions, the increased influence of interface roughness in narrow (10 nm) QWs, spin-orbit effects for the case of holes in an asymmetric confining potential and the different polarities of gate bias changing the charge state of background impurities. However, both [1] and [2] have focussed on the factors influencing the transport of electrons and holes in relatively high carrier concentration ambipolar devices. It will, therefore, be of much interest to contrast these behaviours in the vicinity of the so-called 2D MIT where localisation and interaction effects [3–6] might be more prominent.

In this article we report measurements of ambipolar transport in an undoped QW device of width $d = 15$ nm in the T interval from 3 K down to 0.3 K in parallel magnetic fields B of up to 10 T, with particular emphasis on the low carrier concentration regime. While several of our results are in agreement with previous studies pertaining to the 2D MIT, suggesting that our ambipolar devices are well-suited to study this remarkable and controversial phenomenon, we encounter a novel re-entrant linear regime in the low-density two-dimensional hole gas (2DHG), wherein the I_{SD} - V characteristics go from being linear to non-linear and then linear again as a function of I_{SD} . This behaviour was observed only at low p and not observed at all for the two-dimensional electron gas (2DEG).

The wafer structure and details of the device fabrication are described in detail in [7]. In brief, the wafer consists of two undoped AlGaAs layers sandwiching a 15 nm undoped GaAs layer along the highly symmetric (100) plane. A 2DEG/2DHG can be induced in the GaAs layer (i.e. quantum well) via a top-gate electrode. Photolithography was used to pattern the wafer into Hall bars of width $W = 140$ μ m and length $L = 1120$ μ m, Ohmic contacts were fabricated as described in [7], and finally top-gate electrodes were deposited to induce and tune the carrier concentration. All measurements reported here were conducted in a He-3 cryostat with a base temperature of 0.3 K with

magnetic fields of up to 10 T. Four-terminal constant current measurements were performed using standard low frequency (≈ 12 Hz) AC lock-in techniques. The rms value of the AC excitation current I_{SD} was varied over a broad range from 0.1 nA to 200 nA. The devices had four voltage probes enabling the measurement of Hall voltage V_{xy} in two parts of sample and/or longitudinal voltage V_{xx} along both sample edges. At high n and p the values from different pairs of voltage probes always coincided. In the following we define the resistance $R \equiv V_{xx}/I_{SD}$, the resistivity $\rho \equiv R \times W/L$ and the Hall resistance $R_{xy} \equiv V_{xy}/I_{SD}$.

Figure 1 shows the dependences of n and p on the top-gate voltage V_{tg} , as inferred from the Hall effect. Where possible, we also measured the dependence of n and p on V_{tg} using Shubnikov de Haas oscillations and at high n and p , the difference between these two measures was found to be negligible. A threshold voltage V_{th} is seen for the population of both electrons and holes which is caused by the fact that at $V_{tg} < V_{th}$ the low carrier density leads to either localisation of carriers or failure of the Ohmic contacts. The low-density end for both the electrons and the holes is zoomed-in and shown as an inset to figure 1. It is seen that the dependences of n, p against V_{tg} for this end deviate from a linear behaviour which may be caused by the start of the carrier localisation.

Figures 2(a) and (b) show the dependence of μ_e and μ_p as a function of n and p measured at $T = 0.3$ K and 1.4 K. One can see that while μ_e is larger, T -independent and increases almost linearly with n , μ_p is smaller, strongly T -dependent and has a maximum at $p \approx 1.5 \times 10^{11}$ cm^{-2} . The different T -dependences stem from the difference in m^* for the electrons and holes: for electrons where $m^* = 0.067m_0$ (with m_0 the bare electron mass), the Fermi temperature $T_F = \pi \hbar^2 n / k_B m^*$ is much larger than that for holes where $m^* \approx 0.5m_0$. For example, even at $n \sim 1 \times 10^{10}$ cm^{-2} (which is lower than is experimentally achieved here), $T_F \sim 4$ K, and thus $T_F > T$ in most of the parameter space explored for electrons, and the Fermi–Dirac distribution is a step

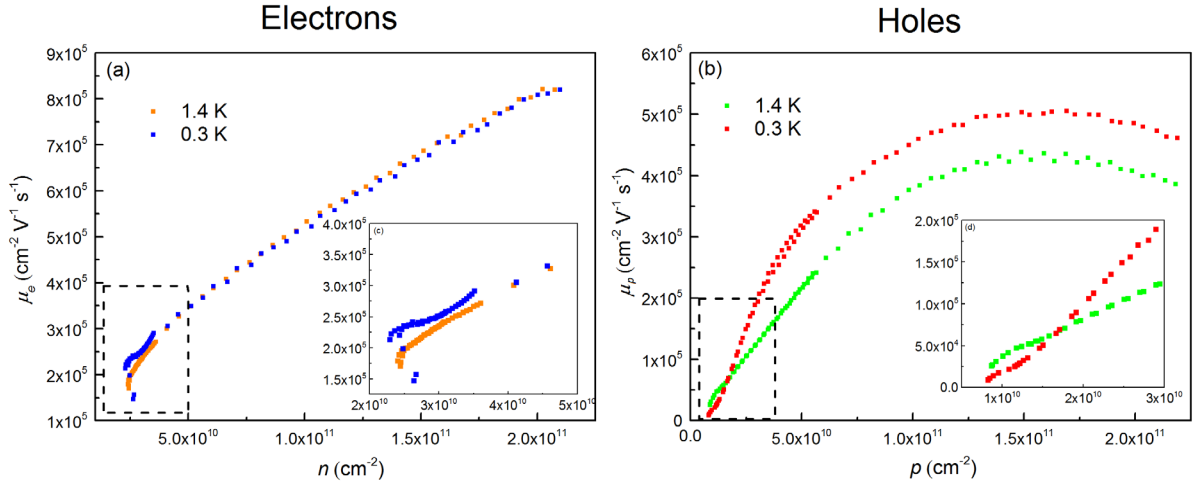


Figure 2. (a) μ_e against n and (b) μ_p against p at $T = 1.4 \text{ K}$ and 0.3 K . The low density regions are zoomed into and shown as insets. Data taken with $I_{\text{SD}} = 100 \text{ nA}$.

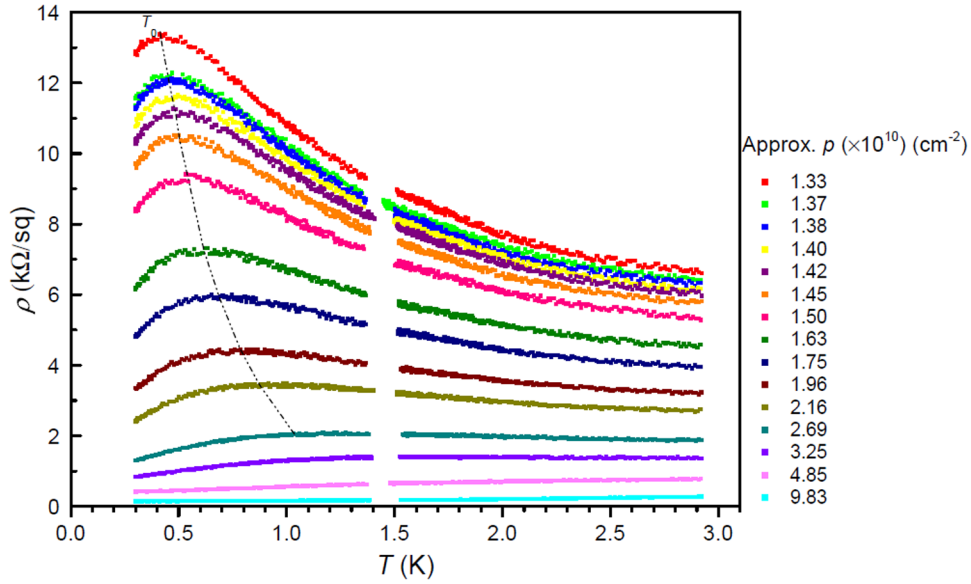


Figure 3. $\rho(T)$ for the 2DHG for various p . Data taken with $I_{\text{SD}} = 10 \text{ nA}$.

function. Correspondingly, the 2DEG resistivity and mobility are largely T -independent. On the other hand, at similar values of p , $T_F \approx 0.5 \text{ K}$, rendering the Fermi–Dirac distribution function smeared over the T -range of interest. This, in turn, opens up a much wider phase space for scattering, and also modifies the screening behaviour of the 2DHG, both of which could yield the observed T -dependence of μ_p .

The observed maximum in μ_p is consistent with previous reports in the literature at similar densities [8–10]. One likely reason for this in the present case could be the increased scattering from interface roughness at high densities, as the hole wave-function is pushed closer to the upper interface [8] with increase of V_{tg} . The impact of the interface roughness scattering for holes is known to be greater than for electrons [2]. Importantly, the observed density dependence of μ_e and μ_p is in qualitative agreement with that reported in [2], where the ambipolar devices had a different design, namely symmetrically placed gate electrodes, above and below the conducting channel, as opposed to a single gate electrode in the devices

reported here. We expect that the asymmetric nature of gating in the present case leads to suppression of μ_e and μ_p relative to that in [2] where through the combined action of both gates, the wavefunction could be centred away from the QW walls.

The T dependences of resistivity $\rho(T)$ for the 2DHG are shown in figure 3 for p varying between $\approx 9.83 \times 10^{10} \text{ cm}^{-2}$ and $\approx 1.33 \times 10^{10} \text{ cm}^{-2}$. Note that this experiment was conducted in two different parts— T was first reduced from 3 K to 1.5 K , and then from 1.4 K to the base temperature of 0.3 K . The data between 1.4 K and 1.5 K are missing due to the difficulty in stabilising T in this range. However, the smooth nature of the traces rules out any problems with thermalisation etc that might prevent the seamless merging of the datasets.

One can see from figure 3 that at $p > 4.8 \times 10^{10} \text{ cm}^{-2}$ $\rho(T)$ is monotonic in the T interval explored, with $d\rho/dT \geq 0$. For $p < 2.7 \times 10^{10} \text{ cm}^{-2}$, however, $\rho(T)$ displays a maximum at a characteristic temperature T_0 with $d\rho/dT < 0$ for $T > T_0$. In other words the 2DHG shows ‘metallic’ behaviour at low T . Such non-monotonic behaviour has been observed earlier in n - and p -GaAs

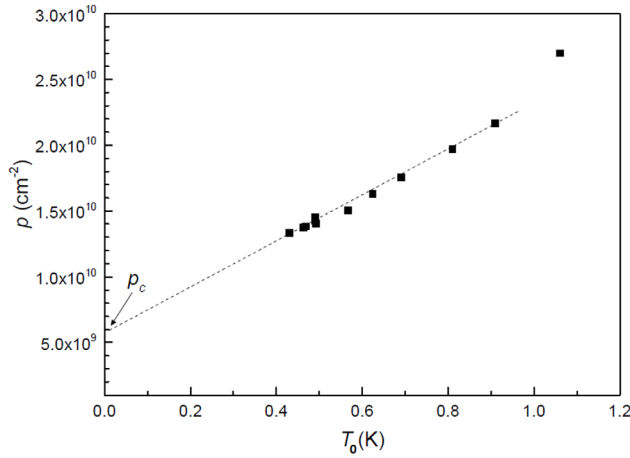


Figure 4. Dependence $p(T_0)$. Extrapolation of the approximately linear dependence to $T_0 = 0$ K gives the rough estimate of the critical density of holes for MIT, $p_c \approx 6 \times 10^9 \text{ cm}^{-2}$. Data taken with $I_{SD} = 10 \text{ nA}$.

heterojunctions and QWs [11–13]. It is found that T_0 depends approximately linearly on p (see figure 4). Although a ‘metal-to-insulator transition’ (MIT) is not observed in our data, it is natural to assume that the critical density p_c is achieved when $T_0 = 0$ K. In figure 4 we find that a rough extrapolation of the p versus T_0 trace gives $p_c \approx 6 \times 10^9 \text{ cm}^{-2}$, which is similar to that obtained in [13] using the same method, for a doped 2DHG confined in a 10 nm wide QW, grown on a (3 1 1) A GaAs surface.

In figure 5 we investigate the behaviour of the 2DHG in the presence of an in-plane B field. As can be seen in figure 5(a), this leads to the suppression of the non-monotonic behaviour of $\rho(T)$, such that $d\rho/dT < 0$ in the entire measured T -interval. Because in-plane fields only affect the spin degree of freedom and not the in-plane orbital motion, this suggests that spin degeneracy of holes is responsible for non-monotonic behaviour of $\rho(T)$ in zero field. Over the entire p range explored, magnetoresistance measurements show that $\rho(B) \sim B^2$ (figure 5(b)) to fields up to 10 T. Notably, no tendency to crossover to linear behaviour, as is expected for a fully spin-polarised 2DHG [14], was observed. The Zeeman energy splitting for GaAs 2DHGs in in-plane fields depends on density, crystal orientation and the shape of the confining potential, due to spin–orbit coupling [15]. Our observation of no full spin polarisation at 10 T is consistent with previous reports from a 15 nm-wide QW on a (100) GaAs surface, where >20 T was required for full spin polarisation [15].

In all measurements described thus far, care was taken to minimise any non-linear effects induced by source-drain electric field $E_{SD} = I_{SD}R/D$ (with R being the sample resistance and D being the distance between voltage probes) and to avoid excessive Joule heating I_{SD}^2R . As these effects become more important with increasing R , Ohmic behaviour was always checked by measurements of the AC $I_{SD} - V$ characteristics especially at low p (where I_{SD} was restricted to $\leq 10 \text{ nA}$). In figure 6(a) we show the $I_{SD} - V$ characteristics at $p \approx 1.25 \times 10^{10} \text{ cm}^{-2}$ which, although are non-linear at $10 \text{ nA} < I_{SD} < 100 \text{ nA}$, appear to crossover to a second linear regime at even higher

I_{SD} . R increases and then saturates at $I_{SD} \approx 200 \text{ nA}$ near a new value about 2–4 times larger than that at low I_{SD} . Qualitatively similar behaviour was observed for all $p \lesssim 1.39 \times 10^{10} \text{ cm}^{-2}$, although the precise interval where the non-linear behaviour is observed varies. Figure 6(b) shows that this second linear regime is observed over a wide range of T . We believe that the small differences in the three traces at the highest I_{SD} reflect fluctuations in p rather than a fundamental change in transport characteristics.

While a departure from Ohmic behaviour at large I_{SD} is entirely expected, it is not at all obvious why Ohmic behaviour should be recovered at even larger I_{SD} . This is clearly not consistent with simply driving the system out of linear response, since higher order contributions ($\propto I_{SD}^n$ with $n > 1$) are expected to grow monotonically. In support of this notion, we were unable to detect a signal at the second harmonic of V_{xx} which provides a measure of terms proportional to I_{SD}^2 . We also note that the behaviour is inconsistent with heating of the 2DHG, as can be seen by comparing figures 3 and 6(b): as the low- p 2DHG is made hotter, ρ decreases (except in the small parameter space below $T \approx 0.5 \text{ K}$). This is precisely opposite to what is observed in figure 6(b). Therefore, while the increased I_{SD} must heat the 2DHG, the associated decrease in ρ appears to be overwhelmed by a competing effect which causes an increase in ρ .

In order to investigate other mechanisms that might enhance ρ , we investigate the dependence of p on I_{SD} . In figure 8 we compare the Hall data for two different I_{SD} and, remarkably we find a distinct reduction in p with increase in I_{SD} especially small $|V_{lg}|$. Thus, our data suggest that the increase in R is not a measurement artefact, or does not arise due to non-linearity/heating effects, but is a direct manifestation of a reduction in the number of carriers at increased I_{SD} . In the following we try to understand this very counter-intuitive observation.

The increase in R with I_{SD} (and hence E_{SD}) is observed most prominently for the low p regime where $\rho \approx h/2e^2$ (as measured with $I_{SD} = 10 \text{ nA}$). At these high ρ the 2DHG is likely to be very inhomogeneous with large fluctuations in the local carrier concentration and background disorder potential. It is reasonable to expect that such large-scale fluctuations in p lead to the appearance of areas where local concentration $p_{loc} < p_c$, the critical concentration of MIT (see figure 7). The closer the average p is to p_c , the larger will be the net coverage of such ‘insulating islands’. From here we suggest that the increase in R and the re-entrant linear regime may be intrinsically related to disorder and inhomogeneity in the 2DHG.

In the following, we present a picture wherein the insulating islands are able to trap free charge carriers in so-called ‘dead ends’ (DEs) (see figure 7), similar to the picture used to understand the ‘negative differential hopping conductivity’ observed in lightly doped Ge [16] and Si [17] (for a review, see [18]).

The original model is based on the idea of DEs in the hopping network or ‘infinite cluster’ along which the current flows in a disordered medium [19]. The DEs can be understood as the end points of percolation paths within an insulating island.

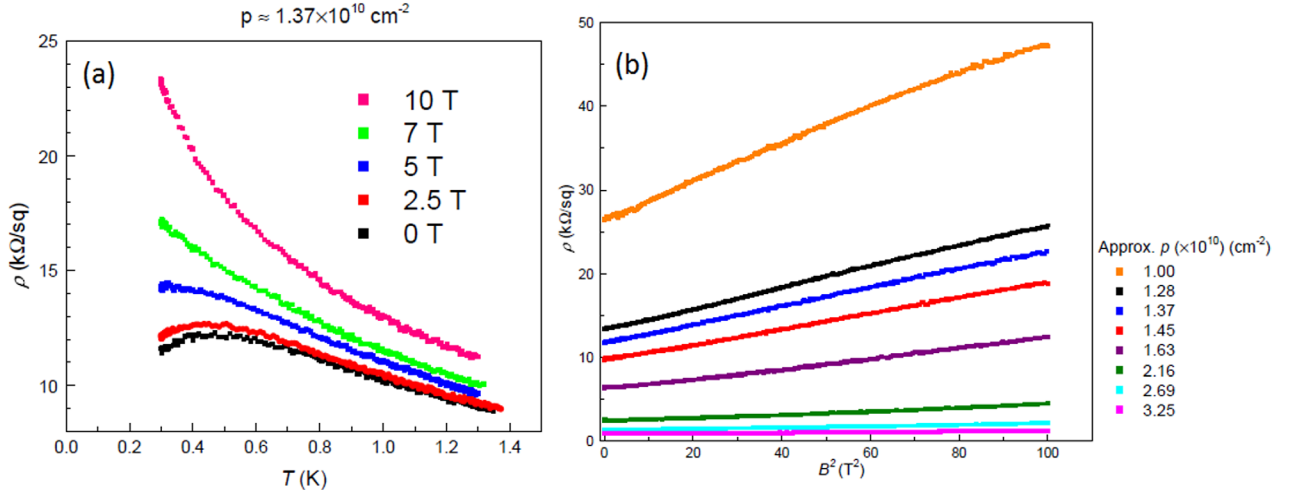


Figure 5. (a) $\rho(T)$ for $p = 1.37 \times 10^{10} \text{ cm}^{-2}$ at different magnetic fields; (b) magnetoresistance versus B^2 for varying p . Data taken at 0.3 K with $I_{\text{SD}} = 10 \text{ nA}$.

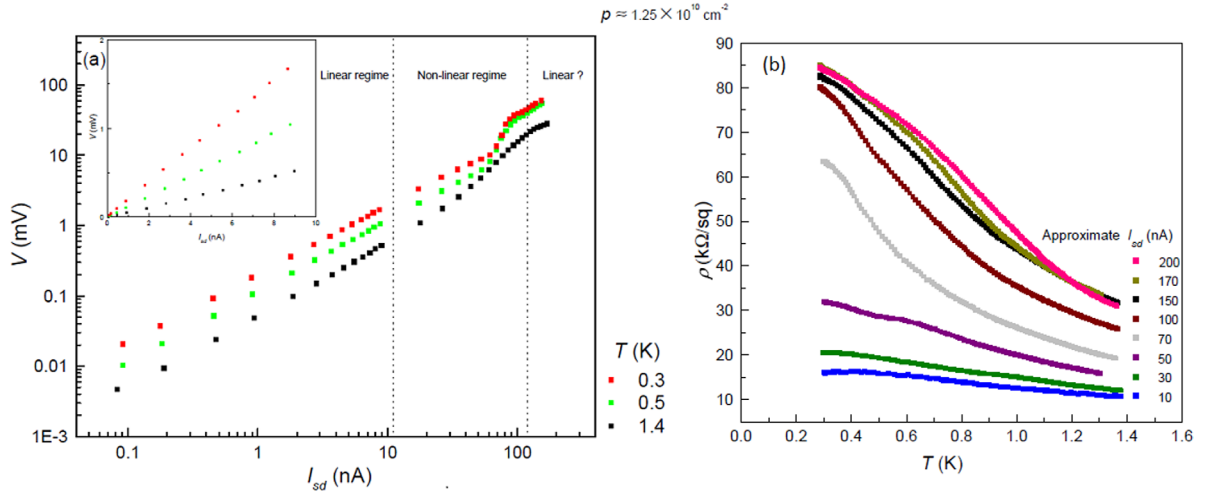


Figure 6. (a) $I_{\text{SD}} - V$ characteristics for $p \approx 1.25 \times 10^{10} \text{ cm}^{-2}$ at $T = 0.3 \text{ K}$, 0.5 K and 1.4 K for I_{SD} varying from 0.1 nA to 200 nA ; the inset shows the low I_{SD} data on a linear scale. (b) $\rho(T)$ behaviour for I_{SD} varying from 10 nA to 200 nA .

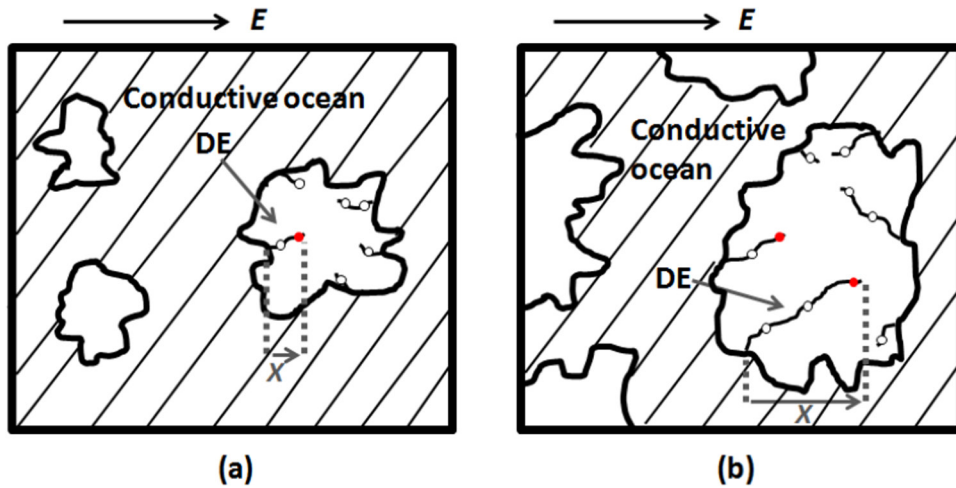


Figure 7. Schematic representation of inhomogeneous conducting layer at low average hole density p barely above the critical density p_c of the MIT. The average carrier concentration p_2 in (b) is smaller than p_1 in (a) and closer to p_c . Insulating islands with $p_{\text{loc}} < p_c$ are shown. The solid points represent charge carriers trapped in 'dead ends' (DE). X indicates the projection of DE along the electric field direction.

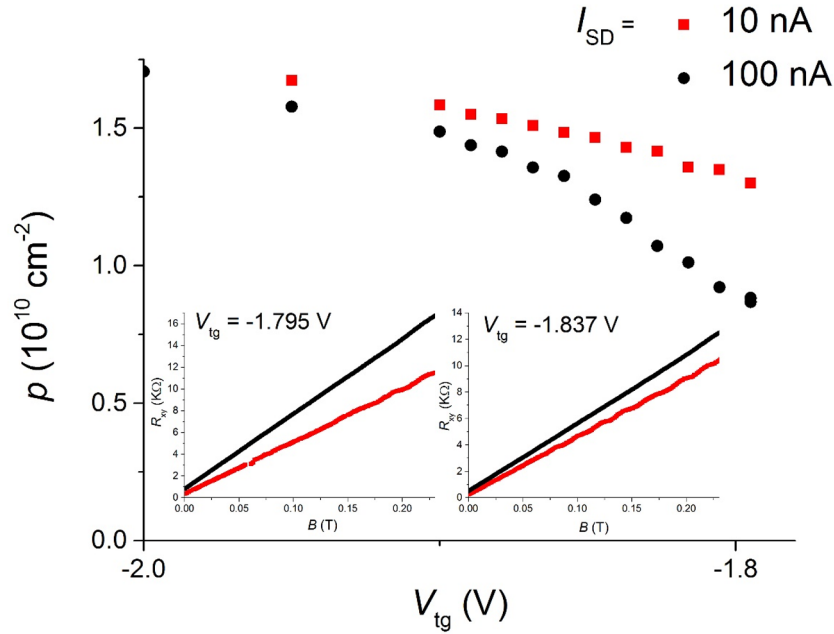


Figure 8. I_{SD} dependence of p versus V_{tg} characteristics. The main panel shows that p is lower for $I_{SD} = 100$ nA, and that the difference between the two traces is largest at low $|V_{tg}|$ where the 2DHG is expected to be inhomogeneous. The p values are obtained from the Hall data, two examples of which are shown as insets. The difference in slope for $I_{SD} = 10$ nA and 100 nA is clearly visible, and the error bars in R_{xy} are smaller than the thickness of the trace. Data taken at 1.4 K.

For a given direction of electric field, charge carriers are able to ‘hop’ along the percolation path until they reach a point which does not have nearby sites to hop to. Obviously, the charge carrier can hop ‘backwards’ along the chain, but for a given direction of electric field, the reverse step is suppressed. The stronger the electric field and/or lower T is, the stronger the trapping effect. This picture clearly demonstrates why a larger electric field serves to suppress rather than enhance conduction. Due to the uneven (likely fractal) nature of the insulating boundary, the DEs are equally distributed in space and orientation, and there is a statistically significant probability of encountering DEs along any arbitrary direction of E_{SD} . For a charge carrier which goes into a DE, there is a probability for it to go out, against the field, which is proportional to $\exp(-eE_{SD}X/k_B T)$, where X is the projection of the length of the DE in the field direction (see figure 7). At weak E_{SD} and high T , this probability is high, close to 1, and charge carriers can go in and out of the DEs easily. However, with an increase of E_{SD} and a decrease of T , the probability of exit decreases rapidly which leads to the trapping of carriers in DEs. With a decrease of average value of p and approaching p_c , the size of insulating areas increases (figure 7(b)) which leads to an increase in number of DEs and their average length X . As a result, the trapping effect is enhanced with a decrease of p and starts at lower I_{SD} . We note that this picture strictly applies only for DC fields, but at the low operation frequencies in the experiments reported here, this picture will apply within each alternating cycle. It is likely that at very short timescales, smaller than the ‘charging/discharging’ time of the DEs, deviations may appear from the behaviour seen in figure 6. However, such high frequency experiments are beyond the scope of the current work. Thus within the picture of DEs, we see that the resistivity ρ is expected to increase with I_{SD} even

within linear response, simply due to the reduction of the net number of mobile charge carriers. This idea is supported by the Hall data in figure 8 which indicates a decrease in p when I_{SD} is increased.

As to why the growth in ρ ultimately saturates, i.e. why there is a second linear regime, beyond a certain threshold value of E_{SD} it can be expected that all appropriate DEs are occupied and trapping of further charge carriers is suppressed by mutual Coulomb repulsion, i.e. the DEs are unable to accommodate further charge carriers. At this point, the DEs stop trapping carriers and increasing E_{SD} has no effect on ρ .

Thus, the ‘DE model’ can explain the key features of our experimental observations of the 2DHG conductivity at low p . In particular, it explains how mobile charge carriers can be rendered immobile in a spatially inhomogeneous system and cause an increase in ρ even without changing T . We stress that this picture does not make any strong assumptions regarding the nature of the 2DHG. In particular, we note that local fluctuation of the carrier concentration are inevitable phenomenon in the vicinity of the MIT and there necessarily exist areas with the local concentration $p < p_c$. Thus we do not expect this effect to depend on the crystal direction and thickness of the quantum well. It will be of interest to re-examine previous experimental literature where such non-linear behaviour may have been relegated to other more mundane effects. That said, at this point it is necessary to consider possible alternative explanations to our data. As described previously, the data is not consistent with heating of the 2DHG or with pushing the system beyond the regime of linear response. There exists a more subtle point, however, which has to do with the manner in which carriers are induced in undoped wafers. In brief, there exists a capacitive coupling between the top-gate (inducing) electrode and the Ohmic contacts which populates

the quantum well with charge carriers. In this context, we draw attention to the fact that in our AC measurement, the voltage at the source contact is oscillating, and thus so is the capacitive coupling with the top-gate. In other words, p is not constant, but undergoes a small alternating modulation in time. To get an estimate of how important this effect is, we consider figures 1 and 6(a). From figure 1 we see that the lowest $|V_{\text{g}}|$ used is ≈ 1.75 V, and from figure 6(a) we see that in the first linear regime ($I_{\text{SD}} \lesssim 10$ nA), the voltage drop across the device is ≤ 1 mV, corresponding to less than 0.1% modulation in the net voltage. Even if one considers the difference $|V_{\text{g}} - V_{\text{th}}|$ rather than the absolute value of V_{g} , we find that this modulation is negligibly small. We note that this effect is only important at low $|V_{\text{g}}|$ where the p versus V_{g} characteristics are not linear; at higher $|V_{\text{g}}|$ the changes in p in the positive and negative voltage cycles will cancel out. At $I_{\text{SD}} \approx 100$ nA, however, the RMS voltage drop across the sample is ≈ 100 mV, which is much more significant, and it can be expected that the large AC amplitude may push the 2DHG quite deep into the localised regime. While this certainly would manifest as an average increase in R as well as reduction in the net number of carriers, it is not obvious that this mechanism would also result in a second linear regime. In other words, we see no reason for this mechanism to saturate with increasing I_{SD} . Thus while this effect may have some influence on the results, we do not believe this to underlie all the observations. In principle, similar arguments apply for 2DEGs as well, although due to differences in screening, effective mass and mobility, these effects might be more difficult to observe in 2DEGs. Within the parameter space explored, we observed no deviation from linear behaviour in the 2DEGs, which might require lower n and/or lower T to manifest.

In conclusion, electron and hole transport are studied in an ambipolar high mobility transistor fabricated on the basis of GaAs quantum well of 15 nm width, enclosed between undoped AlGaAs layers. For holes, non-monotonic dependence of ρ on T was observed within the Ohmic regime of $I_{\text{SD}} - V$ characteristics. It is shown that T_0 , the temperature at which resistivity attains the maximum value, shifts to lower T with decreasing p almost linearly. Extrapolating $T_0(p)$ to $T = 0$ K shows that in our sample, the critical concentration for the MIT $p_c \approx 6 \times 10^9 \text{ cm}^{-2}$. In the presence of a large in-plane B -field, the non-monotonicity in $\rho(T)$ disappears, and ρ monotonically decreases with increasing T . This shows that the zero B non-monotonic behaviour is determined by spin degeneracy of holes. At low p the $I_{\text{SD}} - V$ characteristics are non-linear: R increases with an increase of current I_{SD} (or, equivalently, E_{SD}) and finally saturates at high current. We have suggested an explanation of this effect based on the ‘dead ends’ model, wherein potential fluctuations at low carrier concentrations result in ‘insulating islands’ within the 2DHG that contain ‘dead ends’ which in turn trap a finite fraction of holes.

Acknowledgments

We wish to acknowledge funding from the Engineering and Physical Sciences Research Council (EPSRC), UK. DT acknowledges funding from St. Catharine’s College, University of Cambridge and the Cambridge Philosophical Society. Data supporting this manuscript is available from <https://doi.org/10.17863/CAM.8371>.

References

- [1] Chen J C H, Wang D Q, Klocan O, Micolich A P, Das Gupta K, Sfigakis F, Ritchie D A, Reuter D, Wieck A D and Hamilton A R 2012 *Appl. Phys. Lett.* **100** 052101
- [2] Croxall A F, Zheng B, Sfigakis F, Das Gupta K, Farrer I, Nicoll C A, Beere H E and Ritchie D A 2013 *Appl. Phys. Lett.* **102** 082105
- [3] Koushik R, Baenninger M, Narayan V, Mukerjee S, Pepper M, Farrer I, Ritchie D A and Ghosh A 2011 *Phys. Rev. B* **83** 085302
- [4] Narayan V, Pepper M, Griffiths J, Beere H E, Sfigakis F, Jones G A C, Ritchie D A and Ghosh A 2012 *Phys. Rev. B* **86** 125406
- [5] Narayan V, Pepper M, Griffiths J, Beere H E, Sfigakis F, Jones G A C, Ritchie D A and Ghosh A 2013 *J. Low Temp. Phys.* **171** 626
- [6] Narayan V, Pepper M, Griffiths J, Beere H E, Sfigakis F, Jones G A C, Ritchie D A and Ghosh A 2014 *New. J. Phys.* **16** 085009
- [7] Taneja D, Sfigakis F, Croxall A F, Das Gupta K, Narayan V, Waldie J, Farrer I and Ritchie D A 2016 *Semicond. Sci. Technol.* **31** 065013
- [8] Simmons M, Hamilton A, Stevens S, Ritchie D A, Pepper M and Kurobe A 1997 *Appl. Phys. Lett.* **70** 2750
- [9] Gerl C, Schmult S, Tranitz H P, Mitzkus C and Wegscheider W 2005 *Appl. Phys. Lett.* **86** 252105
- [10] Watson J D, Mondal S, Gardner G, Csáthy G A and Manfra M 2012 *Phys. Rev. B* **85** 165301
- [11] Lilly M P, Reno J L, Simmons J A, Spielman T B, Eisenstein J P, Pfeiffer L N, West K W, Hwang E H and Das Sarma S 2003 *Phys. Rev. Lett.* **90** 056806
- [12] Noh H, Lilly M P, Tsui D C, Simmons J A, Hwang E H, Das Sarma S, Pfeiffer L N and West K W 2003 *Phys. Rev. B* **68** 165308
- [13] Gao X P A, Mills A P, Ramirez A P, Pfeiffer L N and West K W 2002 *Phys. Rev. Lett.* **89** 016801
- [14] Tutuc E, De Poortere E P, Papadakis S J and Shayegan M 2001 *Phys. Rev. Lett.* **86** 2858
- [15] Winkler R, Tutuc E, Papadakis S J, Melinte S, Shayegan M, Wasserman D and Lyon S A 2005 *Phys. Rev. B* **72** 195321
- [16] Zabrodskii A G and Shlimak I S 1997 *Sov. Phys. Semicond.* **11** 430
- [17] Aladashvili D, Adamiya Z, Lavdovskii K, Levin E and Shklovskii B 1990 *Hopping and Related Phenomena* ed H Fritzsche and M Pollak (Singapore: World Scientific)
- [18] Shlimak I 2015 *Is Hopping a Science? Selected Topics of Hopping Conductivity* (Singapore: World Scientific)
- [19] Shklovskii B I and Efros A L 1984 *Electronic Properties of Doped Semiconductors* (Berlin: Springer)